Modeling the effects of black carbon and sulfate composition on CCN activation and albedo

K. Pistone,[1] et al.[2]

Abstract. With the beginning of the Industrial Revolution came a significant increase in anthropogenic atmospheric emissions, including but not limited to aerosols. Two such primarily anthropogenic aerosols are black carbon (BC), found in soot, and sulfate, from SO_2 emissions. Both are often products of combustion processes; however, they differ in that while BC is insoluble as emitted, sulfate is significantly soluble. When BC particles are mixed with sulfate –often produced at the same source– the resulting two-component system is hygroscopic, thus allowing formerly insoluble particles to activate into cloud condensation nuclei (CCN), in accordance with Köhler theory. We simulated a two-component CCN system in which the amounts of insoluble carbon and sulfate were varied. It was found that the CCN number depends on both the amount of sulfate and on initial BC size, and thus both size and sulfate fraction were found to affect the albedo. An increase in regulations of sulfate emissions in recent years has led to a decrease in the sulfate-to-black carbon ratio in some regions, while developing regions may see future increases in both emissions. This, combined with the dependence of CCN number on particle composition and size, may result in a change in activation of black carbon. The effects seen here may have significant implications for climate mitigation strategies.

1. Introduction

Köhler theory dictates that at equilibrium, a particle's potential to activate as a cloud condensation nucleus is a function of the particle's radius and the ambient supersaturation. Activation additionally depends on the chemical composition and properties of the particles in question; when a soluble substance is mixed with a insoluble one, the system becomes more complex.

Black carbon is an insoluble particle that is worthy of particular study because it comes from a variety of primarily anthropogenic sources. Particles containing BC (often called soot) originate from incomplete combustion of carbon-containing material (*Riemer et al.* [2009]), with automobile emissions, biomass burning, and industrial coal combustion as its primary sources. Within these categories, the size and structure of soot particles are additionally dependent on the fuel type, external conditions, and operating condition of their sources (*Huang et al.* [2006], *Bond et al.* [2004]). For example, it is estimated that BC composes ∼70% and ∼20% of US diesel and ordinary gasoline emissions, respectively (*Riemer et al.* [2009]). However, the size, percent composition, and other characteristics of the emissions are highly variable and ultimately difficult to predict, depending on a large variety factors ranging from age and model of the emitter, to technique of the operator and last tuneup (*Bond et al.* [2004]). Overall, *Bond et al.* [2004] estimated in 1996 3.0 Tg/yr of BC from fossil fuel emissions, and 5.0 Tg/yr from biofuel/biomass burning sources.

BC is a strong absorber of solar radiation, and its hydrophobic characteristics make it unlikely for fresh (recently emitted) BC to become CCN; however, when aged, or combined with a hygroscopic substance such as ammonium sulfate through coagulation, condensation, or photochemical processes (*Riemer et al.* [2004]), it becomes possible for BC particles to nucleate into cloud droplets. This is an important value to quantify, as the primary sink for atmospheric aerosols is wet deposition (*Riemer et al.* [2009]), and the life cycle of black carbon both in the atmosphere and when and where it ultimately exits the atmosphere has significant implications for the local and global climate.

In contrast to BC, sulfate is highly hygroscopic and scatters solar radiation for a net cooling effect. Primary sulfur emissions are generally in the form of sulfur dioxide (SO_2) (*Seinfeld & Pandis* [2006]), over 62 Tg/yr from anthropogenic sources, compared with just 2 Tg/yr emitted as sulfate (*Pye et al.* [2009]). Once in the atmosphere, the sulfur dioxide is oxidized to form sulfuric acid (H_2SO_4) and sulfate species (SO_4^{2-}). The latter frequently exists with ammonium as ammonium sulfate, $(NH_4)_2SO_4$, but is henceforth referred to simply as "sulfate". The main source of anthropogenic SO_2 is fossil fuel burning, and to a lesser extent biomass burning. Because of this, it will frequently have the same emission source as BC, providing ample opportunity for the two compounds to interact within an air mass, aging the BC.

There have been several previous studies focused on various aspects of the BC life cycle, both in terms of modeling (*Riemer et al.* [2009], *Kim et al.* [2008], *Kristjánsson* [2002]), and in observational verification (*Schwarz et al.* [2008], *Bond et al.* [2004], *Huang et al.* [2006]). *Kim et al.* [2008] found that in the common method of BC soot aging, low levels of sulfuric acid act as a limiting factor. As the US EPA has determined that sulfate adversely affects the breathing and cardiovascular health of humans, increased regulations (*US EPA* [2009]) have led to reductions in sulfur dioxide emissions in recent decades, particularly in the developed world. At the same time, increased industrialization, particularly in Asia, will likely lead to more (and

[1]Scripps Institution of Oceanography, University of California, San Diego, La Jolla, CA, USA

[2]This work was completed by Kristina Pistone as part of SIO217D term projects created and advised by Lynn Russell, using CCN models originally developed by Greg Roberts, and with the much-appreciated assistance of anonymous and non-anonymous reviewers. However, the submitted work has not yet been reviewed and approved by all of the coauthors and is not suitable for citation at this stage. Please contact Kristina Pistone at kpistone@ucsd.edu to receive an update on these results.

0148-0227/09/$9.00

physically larger) emissions of both BC and sulfur species. It is therefore not a trivial question to ask about the nature of this interaction and how it might affect aspects of the hydrologic cycle, radiation budget, or other climate processes. One particular question at hand is the Twomey effect, which states that an increase in droplet number will result in an increase in optical thickness, thus increasing the albedo. The effect of a change in composition on CCN number and droplet size will be discussed in later sections.

2. Methods

As is necessary when using models, some assumptions and idealizations have been made. In all models used here, the solubility of sulfate is idealized to be infinite, and that of BC is idealized to be 0. Ammonium sulfate is also idealized to be completely dissociative (van't Hoff = 3), and BC is completely non-dissociative (van't Hoff = 0). Finally, the carbon core is idealized as a spherical particle, though this is an oversimplification. Compositional fraction of the system (f_c and f_s) and radius of the composite particle are specified, the former being set by the user, the latter being calculated as described below.

In this model, the dimensions of black carbon are assumed to be constant, with a constant density $\rho_c = 2$ g cm^{-3} following *Schwarz et al.* [2008]. The most accurate model for this system is a black carbon core of radius r_c surrounded by a sulfate shell to radius r_s. From basic geometry, mass is given by

$$M_c = \rho_c \left(\frac{4}{3}\pi r_c^3\right) \tag{1}$$

and

$$M_s = \rho_s \left(\frac{4}{3}\pi \left(r_s^3 - r_c^3\right)\right) \tag{2}$$

By definition, the compositional mass fraction is

$$\frac{M_s}{M_c} = \frac{f_s}{f_c} \tag{3}$$

allowing M_s to be calculated from M_c; thus

$$r_s = \left(\frac{3}{4\pi}\left(\frac{M_s}{\rho_s} + \frac{M_c}{\rho_c}\right)\right)^{1/3} \tag{4}$$

The average diameter of BC particles ranges from 23.6 nm (r_c = 11.8 nm) (*Kim et al.* [2008]), to 0.1 − 0.42μm (*Huang et al.* [2006]), and 200 nm (volume-equivalent diameter, *Schwarz et al.* [2008]), from various sources. Model 1 is a multi-component Köhler model, with density, solubility, van't Hoff factor, and molecular weight as the independent variables for each particle component. This model was run for eleven d_c values between 24 nm and 1μm, the upper limit for the 'fine' particle range. For each radius, a set of seven Köhler curves were calculated corresponding to different sulfate concentrations (50, 40, 30, 20, 10, 5, and 1%).

In order to describe the setup for Model 2, we consider some emissions data. *Bond et al.* [2004] estimate BC emissions from the combination of fossil fuel and biofuel/biomass emissions to be on the order of 8 Tg/year as of 1996. *Pye et al.* [2009] give a sulfate emission budget of 2.04 Tg S/year, with an additional 29.47 Tg S/year production, with a lifetime of just over 3 days before deposition. *Pye et al.* [2009] also predict a 74% decrease in US sulfur dioxide emissions by 2050, resulting in a decrease in sulfate by up to 77%, or 3.2 μg/m^3. From a starting sulfate fraction of 50%, this would give

$$\frac{f_s}{f_c} = \frac{0.5}{0.5} \Rightarrow \frac{0.115}{0.5} = \frac{0.23}{1} = \frac{0.187}{0.813}$$

for a new f_s of 18.7% (assuming BC emissions stay constant). However, while *Pye et al.* [2009] predict a 75% decrease in SO_2 emissions in the US, they also predict a 34% increase (from 61.2 to 81.8 Tg/yr) globally by 2050 from anthropogenic sources alone. Because of this large range in possible values, three sulfate values –40, 25, and 10%– were chosen to correspond to: no regulation/increase in BC; likely decrease in both SO_2 and BC emissions; and large SO_2 reduction. These values were each modeled with the range

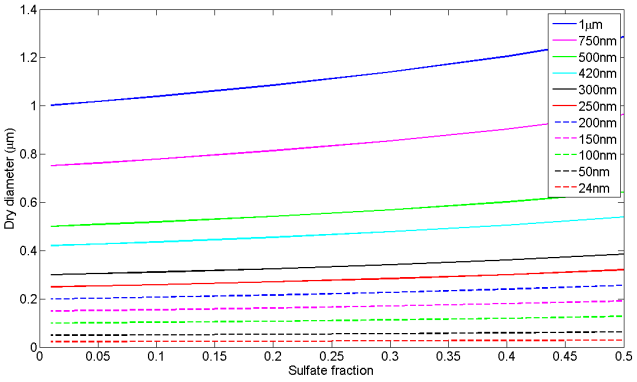

Figure 1. Dry diameter versus percent sulfate for BC diameters from 24 nm to 1 μm.

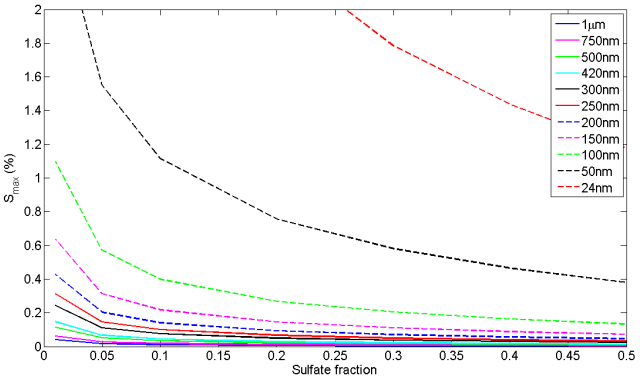

Figure 2. Supersaturation percent S_{max} versus percent sulfate for initial BC diameters from 24 nm to 1 μm.

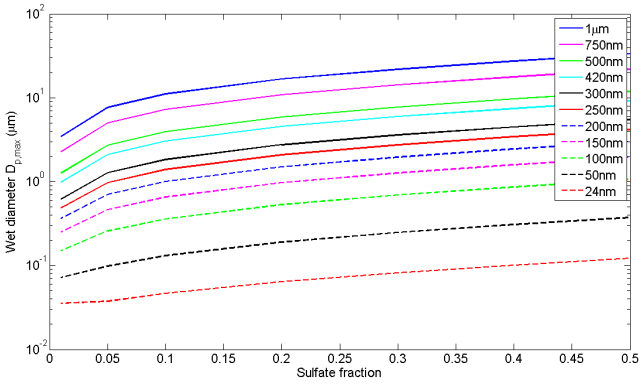

Figure 3. Wet particle diameter $D_{pk,max}$ (μm) versus percent sulfate for initial BC diameters from 24 nm to 1 μm.

of BC core sizes found in literature: 0.42 μm, 200 nm, 100 nm, and 24 nm. However, because emissions of larger BC particles have been linked to economic status (*Bond et al.* [2004]), both in a global context and within a given region, one must keep in mind that real-world smaller BC particles –better technology and education– will likely correspond to lower sulfate values.

The above values, combined with the results of Model 1, are used in Model 2, which generates a lognormal size distribution (dN dlogD$_p$ as a function of diameter in μm) and plots the fraction of particles that are activated into CCN for a given supersaturation, given an initial number concentration N (cm^{-3}), median diameter D$_p$ (μm), standard deviation σ, and soluble fraction k_s. The standard deviation of each scenario is taken to be $\sigma = 2$. Model 2 performed these calculations for the four BC diameters and three sulfate values from above, with values of d_{dry} as calculated by Model 1.

A final model, Model 3, was run to obtain the optical depth τ. *Twomey* [1977] approximated the optical depth for a given size distribution by

$$\tau = 2\pi N \hat{r}^2 h \tag{5}$$

where N is the number of droplets per cm^{-3}, $\hat{r}$ is the mean radius, and h is the thickness of a given mass. The output N from the previous model is combined with $r_{pk;wet}$ from the first model to calculate τ. Results of all models are discussed in the following section.

3. Results

Figures 1 through 3 illustrate the results of Model 1. Figures 1 and 2 show the initial dry diameter of the particle and the critical supersaturation, respectively, as functions of sulfate fraction for different sizes of carbon cores (between 24 nm and 1 μm). Figure 2 illustrates that for realistic atmospheric values ($S_{max} \leq 1\%$, *Seinfeld & Pandis* [2006]), some sizes and fractions will never activate, specifically 24 nm for sulfate $\leq 25\%$, or for 50 nm with sulfate $\leq 5\%$. For an ambient supersaturation of 0.5% and particles greater than d_{dry} ~100 nm, the composite particles will likely activate with sulfate at a 1:9 ratio by mass with the amount of black carbon (i.e. 10% sulfate, 90% BC). However, it is also clear that this threshold sulfate fraction drops off rapidly with smaller radii –down to 40% for a 50 nm particle– and for supersaturations of less than 1.2%, activation would be impossible altogether for the 24 nm particle described in *Kim et al.* [2008]. Figure 3 illustrates how the peak diameter changes at a near-constant rate for different-sized particles but constant sulfate fraction. The most notable feature of this plot is that the $D_{pk,max}$ changes more rapidly for small concentrations of sulfate. This suggests that a small reduction in already-reduced sulfate would have a larger effect on reducing droplet size than would initial reductions in sulfate; this will be more pronounced for larger particles. However, this is coupled with the strong dependence of S_{max} on sulfate fraction (Figure 2) which could prevent smaller particles from becoming CCN in the first place.

Figure 4 is the result of Model 2, and shows fraction of particles activated for a given sulfate fraction as a function of supersaturation percent for the cases $d_c = 24$ nm, 100 nm, 200 nm, and 420 nm. The plots show the number of particles activated from a normal distribution centered around these diameters with $\sigma = 2$. Three main points can be noted from

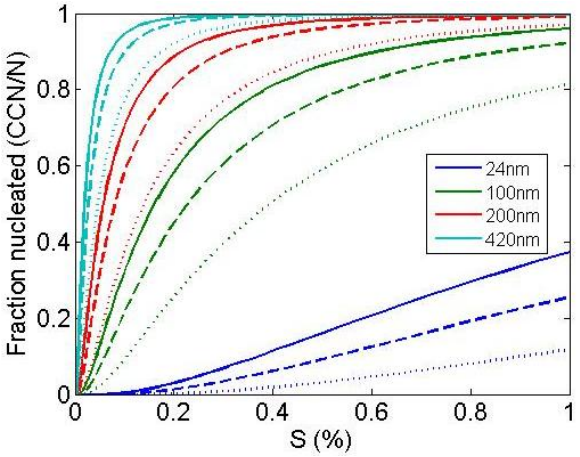

Figure 4. Supersaturation for normal distributions centered around the given diameters. The sulfate percentages are 40% (solid lines), 25% (dashed lines), and 10% (dotted lines).

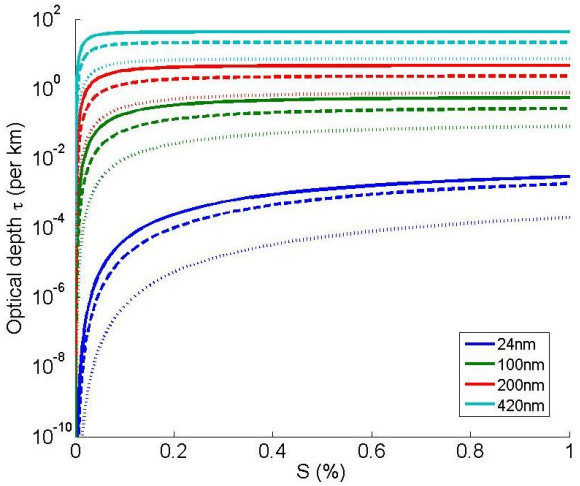

Figure 5. Optical depth τ as approximated by the Trabert-type formula given by *Twomey* [1977] for 40% (solid lines), 25% (dashed lines), and 10% (dotted lines) sulfate.

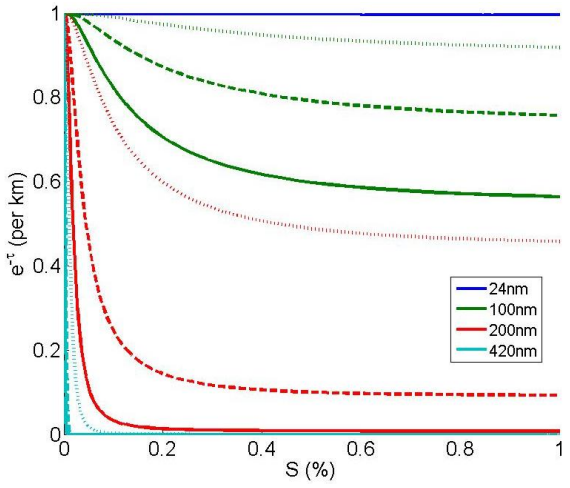

Figure 6. Transmittance through 1 km of atmosphere $e^{-\tau}$ for 40% (solid lines), 25% (dashed lines), and 10% (dotted lines) sulfate.

this plot: first, the number of activated particles has a very strong dependence on initial diameter. This is particularly evident in the 24 nm curve, where for a supersaturation of 1%, less than 40% of particles will activate, even for 40% sulfate. Second, for a 15% reduction in sulfate from 40 to 25%, the number of CCN decreases less than for a 15% reduction from 25 to 10%. Finally, a reduction in size of initial BC emissions reduces the number of CCN more than a reduction in sulfate, given the same number of particles.

Figures 5 and 6 illustrate the optical depth for each combination of radius and solubility, per kilometer of atmosphere (Model 3). A very strong dependence on the initial radius can be seen in Figure 5, about 6 orders of magnitude between 420 and 24 nm. This is again evident in 6, where the difference is between almost total transmission (24 nm) and total extinction (420nm). The trend of stronger sulfate dependence for lower sulfate concentration continues in both plots.

4. Discussion

It is to be expected that when the fraction of hygroscopic substance is reduced in a multi-component system, the ability of particles to form cloud condensation nuclei will be inhibited. An additional trend is the rather strong dependence of S_{max} and CCN number on both percent sulfate and on the size of the initial BC. Köhler curves for the smaller particles, with a larger surface area-to-volume ratios, are much more strongly-peaked compared to the Köhler curves calculated for the larger particles; this is especially true for small sulfate fraction. This is to be expected, as the larger curvature of the smaller particles offers a greater energy barrier to nucleation, which is again doubly true with low sulfate, i.e. with primarily hydrophobic particles. Figure 2 offers evidence of this.

The change in number concentration as a function of sulfate is a direct result of these dependencies. For particles on the order of 0.42 μm, most BC will nucleate under a supersaturation of $\sim$0.1%; about 80% of particles for just a 10% sulfate concentration. This number declines substantially for subsequently smaller BC particles and lower fraction of sulfate.

An important question is what does a change in CCN number distribution imply for the climate system. Figures 4, 5, and 6 show the Twomey effect: an increase in sulfate gives an increase in nucleation which produces an increase in optical depth and thus a dimming effect. While smaller yet more numerous particles typically exhibit a larger albedo, in this particular case the decreased number of activated particles for the smaller size suggests albedo will decrease. In the context of emissions reductions, this effect will be most important for small- or medium-sized particles or for thin clouds, as for larger particles and thick clouds the system is nearly completely saturated and reduction in sulfate will have little effect. However, for a more complete picture other effects must be considered in addition to the Twomey effect seen here. For example, it has been shown that a nucleated BC particle (i.e. with a coating of water around the core) has absorption enhanced by a factor $\sim$1.6. The magnitude of this effect is determined by the amount of coating (sulfate or water) on the BC core, a result of its index of refraction (*Schwarz et al.* [2008]), which creates an increase in BC absorption for an increase in sulfate. An effect such as this would oppose both sulfate's typical role as a scatterer and its effect on BC nucleation as seen here. Further studies and observations should be made to quantify the magnitude of each of effect.

5. Conclusion

Here, model calculations have been used to investigate the effect of sulfate on the ability of black carbon particles to nucleate. It was found that the critical supersaturation has strong dependence on both sulfate fraction and on initial particle size, especially for both lower values of sulfate and smaller BC cores. This relation gives a decreasing CCN number for both decreasing BC particle size and for decreasing sulfate fraction. Considering the Twomey effect alone, this gives a decrease in optical depth for a decrease in sulfate, and thus a decrease in albedo, for a probable warming effect.

Changes in quantity or size of CCN particles affect both the ability of BC to absorb radiation and its role and lifetime in the hydrologic cycle. However, overall it is suggested that a decrease in sulfate will produce a decrease in this enhanced absorption effect, which will result in an increase in reflection or albedo from these particles, counteracting the results found here.

The myriad nonlinear effects resulting from anthropogenic emissions and changes –increase or decrease– to them is an area worthy of study. Ultimately, due to the large range of possible conditions and physical and chemical effects not addressed here, additional observational studies should be done to determine what will dominate for a given set of conditions.

References

Bond, T.C., D.G. Streets, K.F. Yarber, et al. (2004), A technology-based global inventory of black and organic carbon emissions from combustion, *J. Geophys. Res.-Atmos.*, 2004, 109, D14, Jul 24.

Bond, T. C., E. Bhardwaj, R Dong, et al. (2007), Historical emissions of black and organic carbon aerosol from energy-related combustion, 1850-2000, *Global Biogeochem. Cycles*, 21, GB2018, doi:10.1029/2006GB002840.

Huang, X.F., J.Z. Yu, L.Y. He, and M. Hu (2006), Size Distribution Characteristics of Elemental Carbon Emitted from Chinese Vehicles: Results of a Tunnel Study and Atmospheric Implications, *Environ. Sci. Technol.*, 40, 17, 5355-5360.

Kim, D., C. Wang, A.M. Ekman, M.C. Barth, and P.J. Rasch (2008), Distribution and direct radiative forcing of carbonaceous and sulfate aerosols in an interactive size-resolving aerosol-climate model, *J. Geophys. Res.-Atmos.*, 113, D16, Aug 28, ISI:000258821800005.

Kristjansson, J.E. (2002), Studies of the aerosol indirect effect from sulfate and black carbon aerosols, *J. Geophys. Res.-Atmos.*, 107, D15, Aug.

Pye, H. O. T., H. Liao, S. Wu, L. J. Mickley, D. J. Jacob, D. K. Henze, and J. H. Seinfeld (2009), Effect of changes in climate and emissions on future sulfate-nitrate-ammonium aerosol levels in the United States, *J. Geophys. Res.*, 114, D01205, doi:10.1029/2008JD010701.

Riemer, N., H. Vogel and B. Vogel (2004), Soot aging time scales in polluted regions during day and night, *Atmos. Chem. Phys.*, 4, 1885-1893, Sep 15.

Riemer, N., M. West, R. A. Zaveri, and R. C. Easter (2008), Simulating the evolution of soot mixing state with a particle-resolved aerosol model, arXiv:0809.0875v1, 4 Sep 2008.

Riemer, N., M. West, R. Zaveri, R. Easter (2009), Estimating black carbon aging time-scales with a particle-resolved aerosol model, arXiv:0903.0029v1, 28 Feb 2009.

Schwarz, J.P., J.R. Spackman, and D.W. Fahey et al. (2008), Coatings and their enhancement of black carbon light absorption in the tropical atmosphere, *J. Geophys. Res.-Atmos.*, 113, D3, Feb 14

Seinfeld, J. and S. Pandis (2006), *Atmospheric Chemistry and Physics, Second Edition.*

Twomey, S. (1977), Influence of Pollution on the Shortwave Albedo of Clouds, *J. Atmos. Sci.*, 34, 7, 1149-1152.

United States Environmental Protection Agency, Criteria Pollutants, http://www.epa.gov/air/oaqps/greenbk/o3co.html, retrieved 30 April 2009. Last updated 13 March 2009.

K. Pistone, Scripps Institution of Oceanography, University of California, San Diego, 9500 Gilman Dr., La Jolla, CA 92092, USA. (kpistone@ucsd.edu)